Characteristics of Self-Assembled Ultrathin Nafion Films

ARTICLE *in* MACROMOLECULES · MAY 2013

Impact Factor: 5.8 · DOI: 10.1021/ma4002319

5 AUTHORS, INCLUDING:

Devproshad K. Paul
The University of Calgary
23 PUBLICATIONS **372** CITATIONS
SEE PROFILE

Aristides Docoslis
Queen's University
55 PUBLICATIONS **981** CITATIONS
SEE PROFILE

Macromolecules

Article

pubs.acs.org/Macromolecules

Characteristics of Self-Assembled Ultrathin Nafion Films

Devproshad K. Paul,[†] Kunal Karan,[†,‡,*] Aristides Docoslis,[†] Javier B. Giorgi,[§] and Joshua Pearce[⊥,∥]

[†]Department of Chemical Engineering, Queen's University, Kingston, Ontario, Canada

[§]Centre for Catalysis Research and Innovation, Department of Chemistry, University of Ottawa, Ottawa, Ontario, Canada

[⊥]Department of Mechanical and Materials Engineering, Queen's University, Kingston, Ontario, Canada

Supporting Information

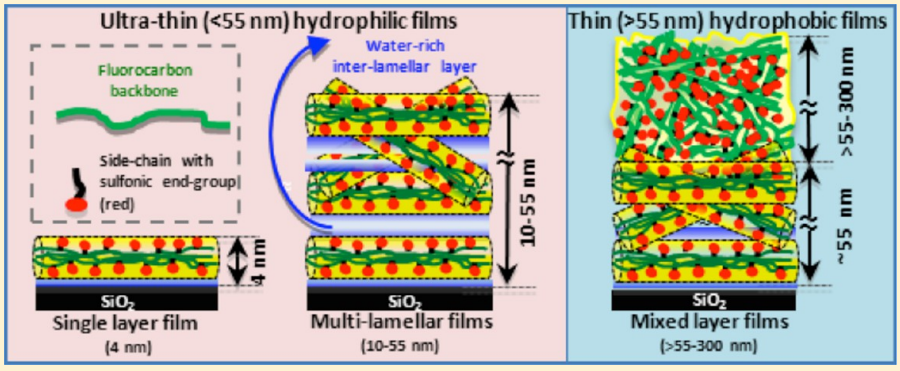

ABSTRACT: Self-assembled Nafion films of varying thickness were generated on SiO_2 terminated silicon wafer by immersion in Nafion dispersions of different concentrations. The impact of solvent/dispersion media was probed by preparing films from two different types of Nafion dispersions—IPA-diluted dispersion and Nafion-in-water dispersion. The thickness of films was ascertained by three different techniques: variable angle spectroscopic ellipsometry (VASE), atomic force microscopy (AFM), and X-ray photoelectron spectroscopy (XPS). The three techniques yielded consistent nominal thicknesses of 4, 10, 30, 55, 75, 110, 160, and 300 nm for films self-assembled from IPA-diluted Nafion dispersions of concentrations 0.1, 0.25, 0.5, 1.0, 1.5, 2.0, 3.0, and 5.0 wt %, respectively. Films generated from 0.25−5.0 wt % Nafion-in-water dispersions generated comparable thicknesses. An interesting finding of our work is the observation of bimodal surface wettability, investigated by water contact angle. The sub-55 nm films were found to exhibit hydrophilic surface whereas the thicker films showed hydrophobic surface similar to those reported for Nafion membranes. Employing XDLVO theory, surface energies of the hydrophobic, 160 nm film was found to be similar to that reported for Nafion membrane whereas those for the hydrophilic 4 nm film yielded high electron-accepting/proton-donating parameters resulting in an enhanced surface polarity. It can be concluded that the structure and properties of the ultrathin (<55 nm) Nafion films are distinct from those of the thicker (but still submicrometer) films, which are likely similar to those of the well-studied Nafion membranes. No significant effect of dispersion type was observed for 10−300 nm thick films.

INTRODUCTION

Nafion is a copolymer with comb-like structure made of fluorocarbon monomer as a backbone upon which the sulfonic acid terminated perfluorovinyl ether monomers are decorated as pendants as shown in Scheme 1.

Scheme 1. Perfluorosulfonic Acid (PFSA) Polymer

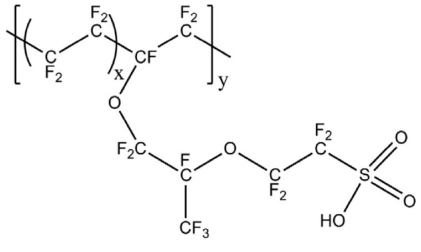

The exact molecular mass of a single chain Nafion molecule is generally not reported; although, values ranging $1 \times 10^5 - 1 \times 10^6$ g have been stated.[1] Instead, the average molecular mass (in grams) per sulfonic group referred to as the equivalent weight (EW) has been employed as an identifier. An EW of 1100 would correspond to x equal to 6 and y equal to 1 in the polymer chain shown in Scheme 1. It is instructive to recognize some of the length scales associated with the molecular structure. From the typical bond lengths, the extended side chain length can be estimated to be of the order of 0.8 nm and the extended backbone spacing between two side chains, uniformly distributed along the backbone, can be estimated to

Received: January 31, 2013
Revised: April 5, 2013
Published: April 22, 2013

Table 1. Summary of Literature on Nafion Thin Films[a]

references	solution properties	substrates	preparation methods	thicknesses	diagnostic tools
Blanchard et al.[10]	5 wt % Nafion (EW = 1100)	ZnSe (IR transparent)	spin coating	100 nm	IR
Krtil et al.[11]	5 wt % Nafion diluted 40 times by methanol (EW = 1000)	silver electrode of QCM	drop casting	20 nm, 80 nm	AFM, QCM
Hill et al.[12]	1 wt % Nafion in 1:1 C_2H_5OH:H_2O mixture (EW = 800)	SiO_2 /Si wafer	self-assembly by immersion for 5 min	200 nm, 400 nm	AFM, STM
Bertencello et al.[13]	5 wt % Nafion diluted by 9:1 CH_3OH:H_2O, filtered through 0.5 mm membrane filter (EW = 1100)	ITO, quartz slides, mica, Au	Langmuir−Schaefer	1.3 −16 nm	UV−vis, QCM, CV
Siroma et al.[14]	5 wt % Nafion diluted by 10−20 times by ethanol (EW = 1000)	Si substrate with Pt band electrode	drop casting	70 nm	EIS
Ugo et al.[15]	5 wt % Nafion diluted by methanol (EW = 1100)	silanized ITO, thiolated Au	Langmuir−Blodgett	5.25−11.3 ug/cm^2	IEV, QCM
Bartencello et al.[16]	dilution of commercial Nafion by methanol to 0.85 mg/mL (EW = 1100)	SiO_2	Langmuir−Schaefer	16 nm	SEM, CV, AFM
Umemura et al.[17]	5 wt % Nafion (EW = 1100)	metal (unspecified) disk	drop casting	230 nm	AFM
Murthi et al.[18,19]	20−22 wt % Nafion diluted 16:1 by anhydrous C_2H_5OH (EW = 1000)	native SiO_2, thermal SiO_2Au, Pt	spin coating, annealing at 60 °C	50 nm	NR
Wood et al.[20]	Nafion solution-concentration not specified (EW = 1100)	Glassy Carbon (GC), Pt-coated GC, Si wafer	Spin coating, Either cured at 140 °C or annealed at 210 °C	60 nm	NR, voltammetry
Noguchi et al.[21]	Nafion (EW = 1020)	Quartz prism	Spray deposition	500 nm	SFGS
Siroma et al.[22]	5 wt % Nafion diluted by 10−20 times by ethanol (EW = 1000)	Si substrate with Pt band electrode	Drop casting	14−1121 nm	AFM, EIS
Bass et al.[23]	5 wt % Nafion (EW = 1100)	Si wafer	spin coating, annealed at 200 °C overnight	100 nm	GISAXS, contact angle, AFM
Bass et al.[24]	5 wt % Nafion (EW = 1100)	OTS-modified Si wafer	spin coating, annealed at 160 °C for 3−5 days	100 nm	GISAXS, AFM
Paul et al.[25]	5 wt % Nafion diluted by isopropyl alcohol into 1 wt % (EW = 1100)	SiO_2/Si wafer	Adsorption (self-assembled)	50 nm	AFM, EIS
Kongkanand[26]	21 wt % Nafion DE2020 diluted to 0.03−3 wt % (EW = 950)	Au, Pt	drop cast, Annealed at 80 °C	30−300 nm	QCM
Ahmed et al.[27]	5 wt % Nafion diluted by a factor of 1000 with ultrapure water (EW = 1100)	Pt (111, 311, 511, and 711)	adsorption	3.3 nm	CV, XPS
Dishari et al.[28]	20 wt % Nafion diluted by ethanol into 2, 5, and 10 wt % (EW = 1100)	Si wafer	spin coating	70−600 nm	QCM
Modestino et al.[29]	5 wt % Nafion diluted by 2-propanol into 2% Nafion solution (EW=1100)	SiO_2/Si wafer, OTS-modified Si wafer	spin-cast, annealing at 200 °C	100 nm (approximately)	GISAXS, ellipsometer
Eastman et al.[30]	20% Naftion was diluted to varied extents with anhydrous ethanol (1:20 to 1:4 by volume)	Si wafer	spin coating	approximately 20−222 nm	GISAXS, QCM, NR, PM-IRRAS, SXR

[a]IR: infrared spectroscopy. AFM: atomic force microscopy. QCM: quartz crystal microbalance. NR: neutron reflectometry. CV: cyclic voltammetry. EIS: electrochemical impedance spectroscopy. SFGS: sum-frequency generation spectroscopy. UV: ultraviolet−visible spectroscop. STM: scanning tunneling microscope. SEM: scanning electron microscope. GISAXS: grazing incidence small angle X-ray scattering. EIS: electrochemical impedance spectroscopy. IEV: ion-exchange voltammetry. PM-IRRAS: polarization−modulation infrared reflection−absorption spectroscopy. SXR: specular X-ray reflectometry.

dx.doi.org/10.1021/ma4002319 | Macromolecules 2013, 46, 3461−3475

be of the order of 0.6−1.2 nm for Nafion of EW of 1100.[2] Accordingly, the length of a single extended molecule with a molecular mass of 1×10^5 g would be in the order of 100 nm, and indeed, an extended molecule may not be expected in solutions or solid state.

Self-standing films (thickness >25 μm) of Nafion are considered to be the benchmark electrolyte membrane for polymer electrolyte fuel cells (PEFCs) and also find applications in chlor−alkali and water electrolyzers.[3,4] Much thinner, supported films of Nafion are finding increasing applications in sensors and actuators.[5] An interesting thin-film structure, not yet fully understood, arises during the self-assembly of Nafion on aggregated Pt/C catalyst during the catalyst ink formulation stage of PEFC electrode fabrication resulting in ultrathin, discontinuous films on nonplanar, heterogeneous substrate.[6] The thickness of these films are less than 10 nm, much larger than the side chain length and much smaller than the extended length of a single molecule.

The membrane form of Nafion (>25 μm) has been studied extensively over the past several decades;[7] although, the nanoscale structure still remains a topic of debate.[8,9] In contrast, few studies on ultrathin and thin films (mostly 50 nm to several hundreds of nanometer) of Nafion have been reported.[10−30] The structure and properties of the thin and ultrathin Nafion films are even less understood. Here, we adopt the terminology[31] for polymer films where films of less than 100 nm thickness are deemed to be ultrathin film, and those with thickness greater than 100 nm but less than a micrometer deemed to be thin film. For Nafion, an emerging body of knowledge indicates[18,19,22−26,32] that the properties of the ultrathin and thin films may differ significantly from those of the membrane form of Nafion.

A summary of key studies in the literature on thin/ultrathin Nafion films is provided in Table 1. The studies differ in the choice of solution/solvent characteristics, the type of substrate used and the film fabrication/processing methods − all of which may impact the film properties. Spin coating and drop casting appear to be the most common methods for film preparation resulting in film thickness typically greater than 50 nm although films as thin as 14 nm have also been reported.[22] Using Langmuir−Schaefer and Langmuir−Blodgett methods,[14−16] fabrication of even thinner films has been attempted.

A variety of substrates have been used for film preparation including SiO_2-terminated silicon wafers,[12,13,16,18,19,22,23,25,28,30] modified silica,[24,29] metals,[10,11,17,19,26,27] and carbonaceous substrates.[20] Recent studies using neutron reflectometry (NR)[18,19] and GISAXS techniques[23,24,29] have found that the substrate has a significant influence on the film structure. From the findings of the NR studies,[19] Nafion films on SiO_2 substrate were proposed to have a multilamellar structure comprising alternate layers of water-rich and Nafion-rich layers whereas Nafion films on Au or Pt surfaces were proposed to have a partially hydrated, single interfacial layer. One GISAXS study[24] concluded that the films had an inverted micellar nanostructure aligned parallel onto a hydrophilic silica substrate but aligned perpendicularly onto a hydrophobic octadecyltrichlorosilane (OTS) modified silica substrate.[24] In another GISAXS study,[29] it was noted that the ionomer channels orient parallel to hydrophobic substrate and not perpendicular as was found in the study of Bass et al.[24] The differences in the structure could arise from sample preparation and treatment. Few studies on the bulk characteristics of Nafion thin films including water uptake measurements[26,28] and proton conductivity[22,25] have been published. Contrasting findings on water uptake have been reported. One study[26] reported that a 33 nm Nafion film has slightly lower water uptake compared to the much thicker 500 nm film whereas another study[28] reported that the 70 nm thick film had much higher water uptake than 600 nm thick film. The lower water uptake by thinner films[26] is consistent with the lower proton conductivity of thinner films reported by Siroma et al.[13,22] and our group[25] for thin Nafion films supported on SiO_2. Most recently, Page and co-workers[30] reported properties of submicrometer thin films prepared by spin-coating on SiO_2. Films of different thicknesses were generated by spin coating from Nafion solutions of varying concentrations prepared by dilution of stock solution by addition of ethanol. A very interesting aspect of their study was the finding that the swelling ratio, volumetric water fraction, and effective diffusivity of films are relatively constant for spin-coated films thicker than ca. 60 nm but were different for the thinner films.

Although the Nafion thin films are prepared from dispersions/solutions, none of the Nafion thin film studies (Table 1.) have examined the effect of dispersion type or characterized the dispersions. In independent studies, small-angle X-ray scattering (SAXS) data of Nafion dispersions in polar media have been interpreted in terms of rod-like structure.[33−36] The radii vary from 2 to 2.5 nm for dispersion media with polarity ranging pure alcohol to pure water.[35] It has also been argued that the small change in radii depend on the surface tension rather than dielectric constant of the solvent.[36] Other studies, dynamic light scattering measurements of Nafion dispersions both in water[37] and in a water/alcohol[38,39] mixture have been interpreted in terms of a fringed rod-like structure where the dangling chain segments of the rod are incorporated into the other rods. It has been proposed that with increasing Nafion concentration, rod-like particles aggregate through ionic side chains and form secondary ionic clusters.[37−39] Cryo-TEM images of Nafion dispersion in various solvent or solvent mixture show a wide verities of self-aggregation pattern in a particular Nafion dispersion concentration. The TEM images represent a much larger-scale structure, likely associated Nafion, than those probed by SAXS. Polar solvent (water/alcohol) mixture such as MeOH−H_2O and IPA−H_2O contain a mixture of rectangle-like and cube-like structures whereas only rectangular-like structure was observed in EtOH−H_2O solvent.[40] Particularly, for IPA−H_2O mixture solvent, it was found that Nafion aggregated particle size decreased with increasing IPA wt %.[41] The self-assembly behavior of Nafion from dispersions of different polar media is not known.

In this study, we report the (free-surface) characteristics of films prepared by self-assembly of Nafion on SiO_2 surface during extended immersion in Nafion solutions/dispersions of different concentrations. Two different Nafion dispersion types were employed to probe the effect of dispersion media. One set of dispersion was prepared by diluting the 5 wt % Nafion stock dispersion with isopropyl alcohol. The other set of dispersion was Nafion in water dispersion, which was achieved by following the solvent switching technique involving successive distillation. A majority of the results are presented for films made from IPA-diluted dispersions. The thickness of the films was ascertained from three different techniques—AFM analysis of scratched film, variable angle spectroscopic ellipsometry (VASE) and X-ray photoelectron spectroscopy (XPS). The wettability of films was assessed through water contact angle. The surface energies of the film were calculated by application

dx.doi.org/10.1021/ma4002319 | Macromolecules 2013, 46, 3461−3475

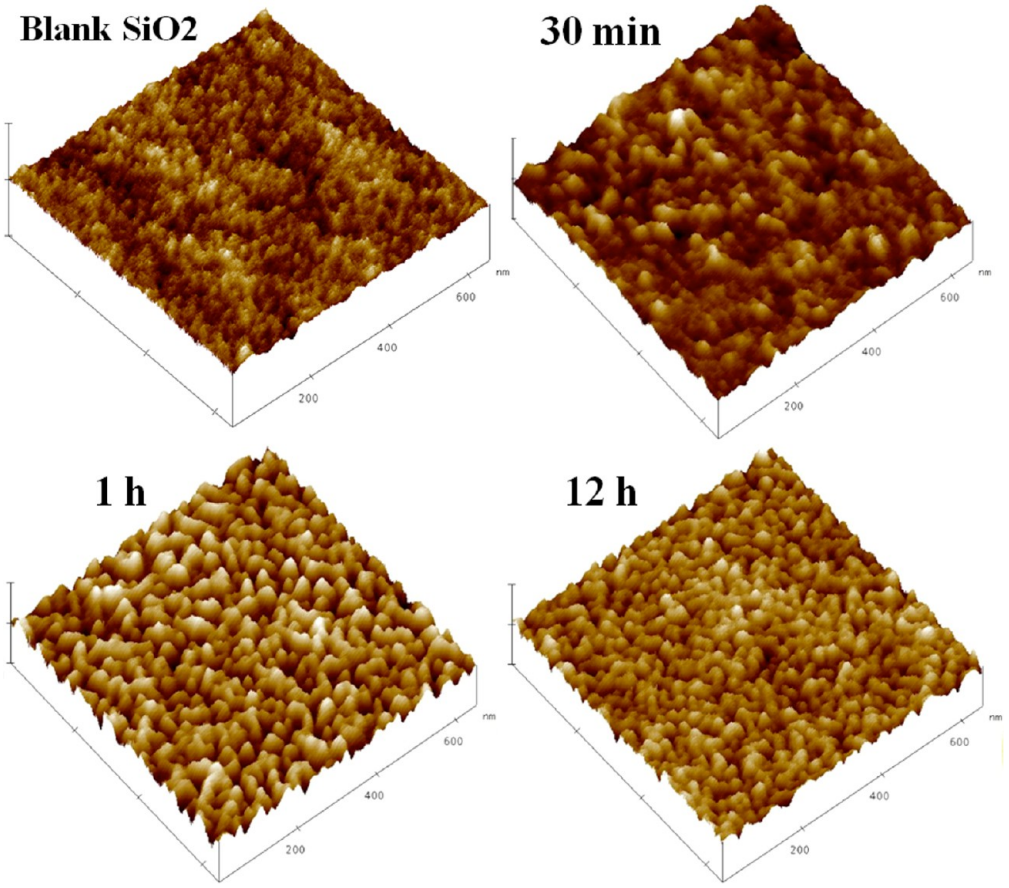

Figure 1. 3-D AFM height images of blank SiO_2 surface (top row left) and of SiO_2 surface after immersion in 0.1 wt % Nafion solution for 30 min (top row right), 1 h (bottom row left), and 12 h (bottom row left).

of extended-DLVO (XDLVO) theory by using contact angle measurements with two additional liquids varying in polarity. The surface morphology of the films were examined by AFM in the tapping mode and analyzed in terms of height and phase contrast. Angle-resolved XPS measurements were conducted to investigate whether any differences in S/F ratio exists in between thinner hydrophilic films and thicker hydrophobic films.

EXPERIMENTAL SECTION

Film Preparation. *Nafion Dispersion Preparation.* Commercially available 5 wt % Nafion (EW 1100) solution in water−alcohol mixture (75/20 w/w alcohol to water) acquired from Ion Power (USA) was used. Like prior studies,[22,28−30] the stock dispersion was diluted to desired Nafion solution by adding an alcohol; although we used isopropyl alcohol instead of ethyl alcohol for dilution. Nafion solutions of concentration 0.1, 0.25, 0.5, 1, 1.5, 2, and 3.0 wt % were prepared by adding appropriate amount of isopropyl alcohol (Sigma-Aldrich) to the stock 5 wt % Nafion solution. Additionally, 5 wt % Nafion dispersion in water was prepared adopting the solvent switching technique described by Moore et al.[42] and Jiang et al.[37] (protocol: see Supporting Information) and followed by dilution by adding Millipore water. The diluted solution was equilibrated at least 24 h after initial 5 min sonication. Dilution followed by long equilibration time was allowed to bring the presumed high aggregation state to its lower aggregation state.

Substrate Cleaning. Silicon wafer with a ∼300 nm thermally grown SiO_2 layer (MTI, USA) was selected as a model substrate. The cleaning of SiO_2/Si wafers involved multiple steps. First, the wafer was exposed to a Piranha (Caution!) solution (H_2SO_4:H_2O_2; 7:3) at 80−90 °C for 1 h to remove surface contamination. Next, the wafer was rinsed with Millipore water and dried under flow of compressed air. Subsequently, the wafer was placed into an RCA (Radio Corporation of America) cleaning solution mixture (DI H_2O:NH_4OH:H_2O_2; 5:1:1) at 70−80 °C for 30 min to remove organic contaminants from the surface. Finally, the wafer was washed by Millipore water several times and dried again under flow of compressed air. The cleanness of the wafer was confirmed by AFM and XPS analyses.

Self-Assembly. Thin films of Nafion were generated by self-assembly of Nafion onto the cleaned SiO_2/Si substrate. The cleaned substrate was immersed in the Nafion solution of known concentration contained in a capped beaker. The substrate was exposed to Nafion solutions for 12 h or otherwise specified time. After carefully removing the substrate from the solution it was dried under a flow of dry air. Vacuum drying was carried out in low vacuum (−30 in. of Hg) at 40 °C for 16−20 h.

Film Characterization. *Atomic Force Microscopy (AFM).* AFM was used to investigate the surface features (morphology, roughness and phase contrast) of the blank substrate and the Nafion thin films. The film thickness was determined by AFM using a line analysis of the film that was scratched all the way through to the SiO_2 substrate. The AFM measurements were performed at ambient conditions in tapping mode using a Nanoscope IIIa system (Digital Instruments) with a silicon tip (tip radius <10 nm) mounted on the cantilever.

X-ray Photoelectron Spectroscopy (XPS). X-ray photoelectron spectra were obtained on a Kratos AXIS UltraDLD 39−306l instrument using a monochromated Al source (1486.6 eV). All the spectra were obtained with constant pass energy of 80 and an energy step of 200 meV. The pressure of the vacuum system was maintained at ∼2×10^{-10} Torr. Samples were introduced into the vacuum system immediately before measurement, minimizing the time in vacuum (atmosphere to measurement ∼40 min), which might change the film's morphology. To prevent excessive charging, a charge neutralizer

dx.doi.org/10.1021/ma4002319 | *Macromolecules* 2013, 46, 3461−3475

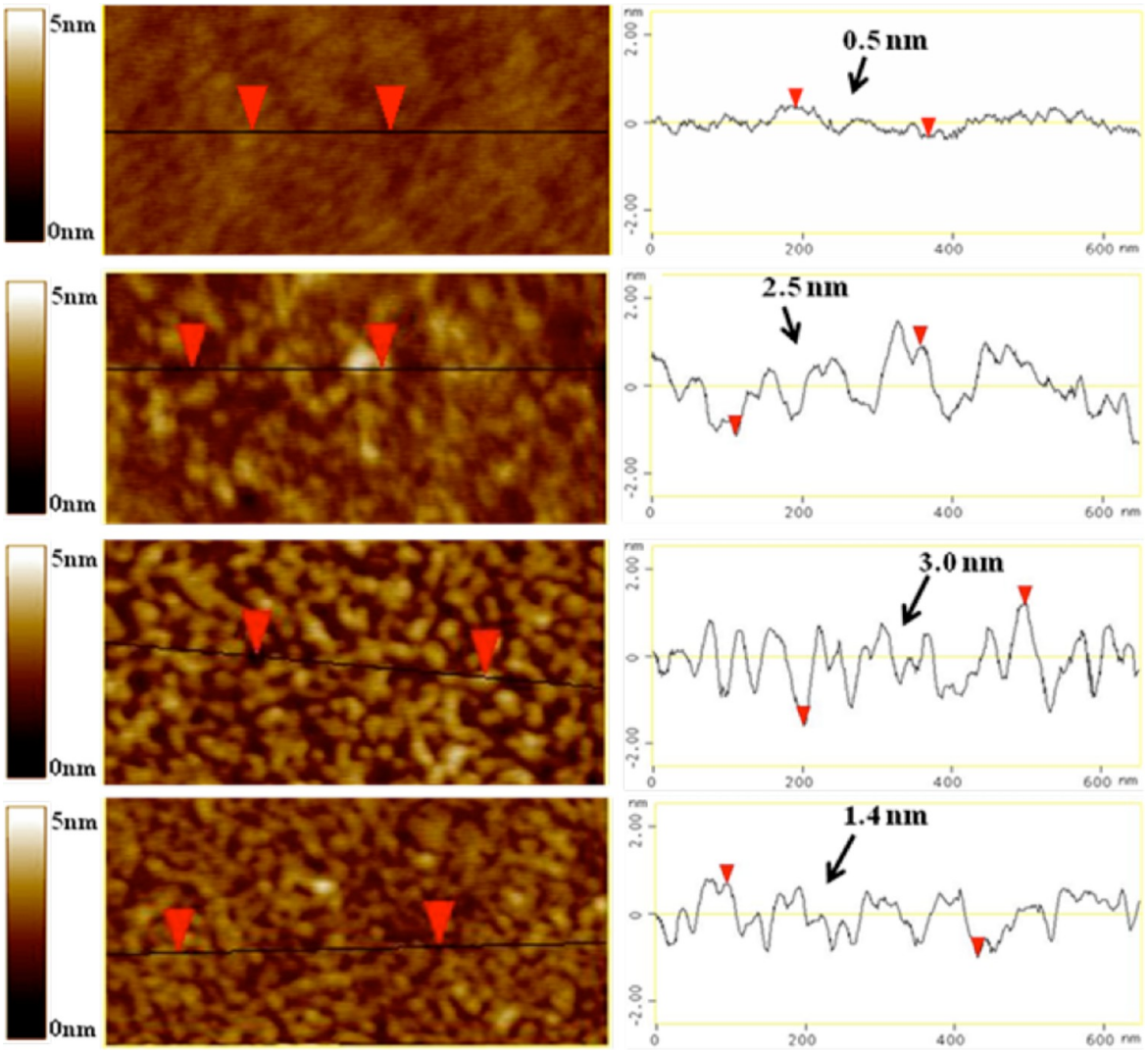

Figure 2. 2-D height images with section analysis. Blank SiO_2 surface (top row) and SiO_2 surface after immersion in 0.1 wt % Nafion solution for 30 min (second top row), 1 h (third row), and 12 h (bottom row).

was used. The binding energy scale was further calibrated by setting the Si_{2p} peak to 103.4 eV.[43,44] This value is well within the range for SiO_2 and silicon-supported SiO_2 films [103−104 eV from ref 45] and results in an adventitious carbon peak at ∼284.8 eV. The carbon peak is not used directly because the multiple contributions of the Nafion film produce slight shifts in this peak. Calibration of the instrumental behavior (intensity dependence of the collection solid angle) during angle-resolved measurements was performed using a freshly sputtered copper sample. Elemental quantification of the Nafion films and the underlying silica was determined using the Si_{2p}, S_{2p}, C_{1s}, O_{1s}, and F_{1s} peaks with a Shirley background subtraction in the CasaXPS software.[46]

Contact Angle Measurement. The contact angles (θ) of sessile drops deposited on Nafion films were measured using a Dynamic Surface Analysis system (VCA Optima, AST Products INC.), equipped with a video camera and software (winvca32) for image analysis. To assess hydrophobic or hydrophilic characteristics, Millipore water was used as the liquid. For surface energy calculations, in addition to water, contact angle measurements with another polar liquid (ethylene glycol) and an apolar liquid (diiodomethane) were carried out. For all contact angle measurements, a sessile drop of liquid using a micro syringe was placed on the surface of a vacuum-dried thin film. Several images were captured starting at 5 s after dispensing each sessile drop for up to 5 min. The relative humidity of the environment was not controlled but varied in the 40−50% range. In this study, the reported contact angles are the values obtained at 5 s after the placement of the sessile drop and the average of four replicates on the film surface.

RESULTS AND DISCUSSION

Surface Characterization of Films Generated by Varying Immersion Times. To investigate structural evolution of the Nafion self-assembly, SiO_2 substrates were exposed to 0.1 wt % Nafion solution for different periods of time—0.5, 1.0, 3.0, and 12.0 h—and the surface of Nafion covered substrate were examined by AFM. The samples were subjected to a washing step soon after withdrawal of the substrate from the Nafion solution to ensure that any adhering liquid and weakly held Nafion molecules were removed. The washing step consisted of instantaneously dipping the solution-exposed substrate into a beaker containing the same solvent that made up the Nafion solution. The washed substrate was then dried in a stream of compressed air. The surface features of the films can be gleaned from the 3D representation of the topography as presented in Figure 1

Each image represents the surface of dimension 650 nm × 650 nm. The bar on the left-hand corner of each image represents a scale of 5 nm. From Figure 1, differences in the

dx.doi.org/10.1021/ma4002319 | *Macromolecules* 2013, 46, 3461−3475

film surface morphology can be noted. The substrate exposed for 0.5 h in the Nafion solution appears to be partially covered by Nafion. On the other hand, the AFM image of substrate exposed for 1 and 12 h indicates more Nafion on the surface. Sample line analyses of the film topographical images are presented in Figure 2 and allow us to draw further conclusions about the changing characteristics of the films generated after immersion in Nafion solution for different times. Comparing films generated after 0.5 and 1 h exposure, 1 h film exhibits a periodic feature width (20 to 30 nm) and height (~3 nm) whereas the periodicity is less clear for the 0.5 h film. Both films can be thought to be corrugated surfaces. The 12 h film showed lower feature height (1.4 nm) compared to the 1 h film. This would indicate smoothening of surface due either to restructuring of the pre-existing adsorbed Nafion or to filling of the corrugations by further adsorption of Nafion. Regardless of what the actual process is, it can be deduced that the surface characteristics changes with increased immersion time, indicating that the process of film formation is a self-assembly type phenomenon. It is also useful to mention that repeat measurements on new samples have shown similar results of ~3 nm feature heights in the low exposure time films and much smoother surface with feature heights in the order of 1 nm for 12 h exposure time films.

To quantify the roughness of the blank and Nafion-covered (partial or full) substrate, the film mean roughness is presented in Figure 3. Surface uniformity and roughness of both substrate

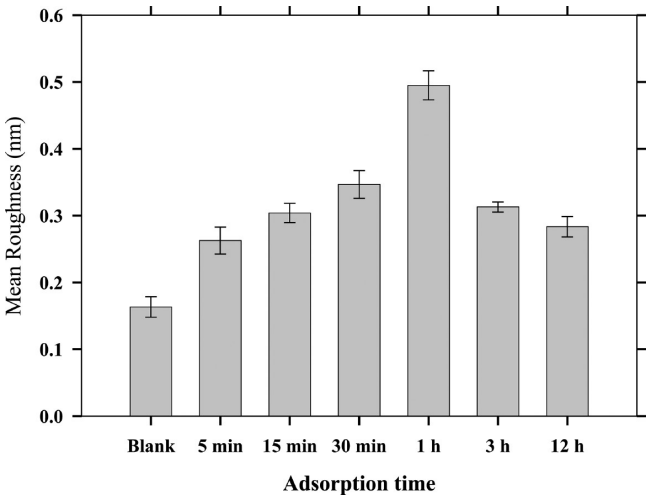

Figure 3. Mean roughness of blank SiO_2 surface and SiO_2 surface immersed in 0.1 wt % Nafion solution for different time.

and films have been parametrized by the mean roughness and root-mean-square (RMS) roughness calculation by the following two formulas:

$$R_m = \frac{1}{NM}\sum_{x=1}^{N-1}\sum_{y=1}^{M-1}|Z_{x,y}| R_{rms} = \sqrt{\frac{1}{NM}\sum_{x=1}^{N-1}\sum_{y=1}^{N-1} Z_{x,y}^{\,2}} \quad (1)$$

Here $Z_{x,y}$ is the difference of height from the mean height; N and M are the number of points in x and y directions. It can be noted that the mean roughness of the films increases from 0.32 nm to nearly 0.5 nm and then decreases to 0.28 nm as the immersion increases from 0.5 to 1 h to 12 h, respectively. The observed trend for mean roughness can be explained by considering the surface coverage and the contribution of the uncovered, covered and edges of the covered regions. Thus, for 0.5 h exposed film, if we consider the substrate is not completely covered, then the mean roughness would be dominated by the bare substrate roughness with additional corrugation due to isolated Nafion molecules. For the 1 h exposed film, the increased roughness can be explained by considering that the number of Nafion molecules on the surface increases, almost completely covering the surface. The 12 h exposed surface shows a reduced roughness due likely to assembly/adsorption of more material. The thickness of 12 h film was measured by scratching the film followed by AFM imaging as shown in Figure 4. The resulting thickness (4 nm)

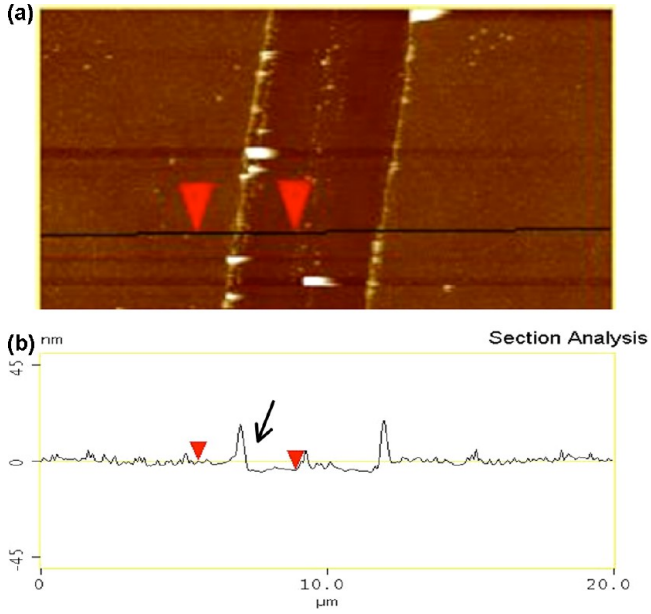

Figure 4. (a) AFM image and (b) line analysis showing height distribution of scratched surface of film deposited from immersion in 0.1 wt % Nafion solution for 12 h.

was more than two times the maximum surface corrugations, which would imply full surface coverage of the Nafion. From the AFM images and line scan data shown in Figure 2, it can be surmised that the 1 h film does not fully cover the substrate. However, no attempts were made to quantify the surface coverage of the films

Thickness of Films Self-Assembled from Nafion Dispersion of Varying Concentrations. Films resulting from self-assembly of Nafion from solutions/dispersions of varying composition were characterized for thickness. Three different techniques—AFM, XPS and ellipsometry—that probe the thickness over different extents of sample size were employed. AFM examined the thickness variation along a scratched length of a micrometer. The spot size for ellipsometry measurements were effectively an area covered by circle of a diameter of 50 μm. XPS measurements averaged the response from the film of an area of 2 mm^2.

Film Thickness by AFM. AFM has been employed to measure thin film thickness successfully using tip-scratch or similar methods.[47,48] Since the self-assembled films were thin, soft and prepared on a sufficiently hard silica substrate, it could be scratched easily all the way though the film thickness by a sharp blade without damaging the hard substrate surface. A line analysis of AFM analysis of the film across the scratched

dx.doi.org/10.1021/ma4002319 | Macromolecules 2013, 46, 3461−3475

portion allows for an estimation of film thickness as shown in Figure 4 for the film deposited from 0.1 wt % Nafion. Similar analyses were performed on films deposited from different Nafion solutions. Several AFM thickness measurements were performed on different regions of each sample to confirm the uniformity of the film thickness. The results of the measurements are reported in Table 2. Because the maximum vertical displacement was limited to 100 nm, the thicker films originating from the substrate immersion in 3 and 5 wt % Nafion solution could not be determined from this technique.

Table 2. Thicknesses of Nafion Films Generated from Different Dispersions and Concentrations

	film thickness (nm)			
	IPA-diluted dispersions			Nafion-in-water dispersion
nafion solution concentration (wt %)	ellipsometry	XPS	AFM	ellipsometry
0.1	4.0	4.3	4	
0.25	10.5	10.5	11	11.6
0.5	31.5	–	32	27.5
1.0	57	–	55	57
1.5	75	–	–	
2.0	110	–	–	
3.0	160	–	–	173
5.0	308	–	–	313

Film Thickness by Variable Angle Spectroscopic Ellipsometry. Ellipsometry measurements were carried out at three incident angles of 55, 65, and 75° over a visible light wavelength range of 350−700 nm. The details of VASE measurements and data analysis were presented earlier.[49] Briefly, results show that the Cauchy model, which considers the Nafion film as a continuous, nonporous layer is appropriate for these films. The Cauchy model is an approximation of the Lorentz type oscillator model for the interaction between the nucleus and the electron clouds. The ellipsometry response, parametrized in terms of ψ and Δ (phase shift), for four different films at an incidence angle of 65° is presented in Figure 5. The Cauchy model considers the film to be homogeneous with an effective refractive index, which along with the film thickness are the model parameters that are fit to the experimental data. The results are presented in Table 2 and thickness data is discussed below.

Film Thickness by XPS. X-ray photoelectron spectroscopy was used to determine film thickness quantitatively and to identify any potential impurities qualitatively in the Nafion film. Three films corresponding Nafion concentrations 0.1, 0.25, and 3.0 wt % were examined. All films showed the correct composition and only in some samples a small peak for trapped nitrogen was observed. Representative XP spectra are presented in Figure 6 for a 0.25 wt % film at different angles.

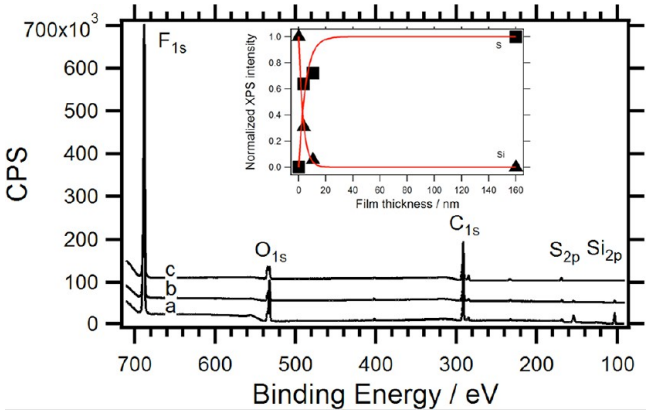

Figure 6. X-ray photoelectron spectra of the 10 nm Nafion film as a function of electron takeoff angle. Key: (a) 90°, (b) 45°, and (c) 10°. Spectra have been offset for clarity. Inset shows the normalized XPS intensity for silicon (solid triangles) and sulfur (solid square) peaks at normal takeoff angle as a function of film thickness.

The inset shows the S_{2p} and Si_{2p} peak intensities normalized with respect to corresponding responses from 3 wt % (160 nm) and bare substrate samples, respectively. The complete disappearance of Si_{2p} intensity from the 160 nm film can be noted.

Evaluation of film thickness was performed using two methodologies to account for potential inconsistencies or

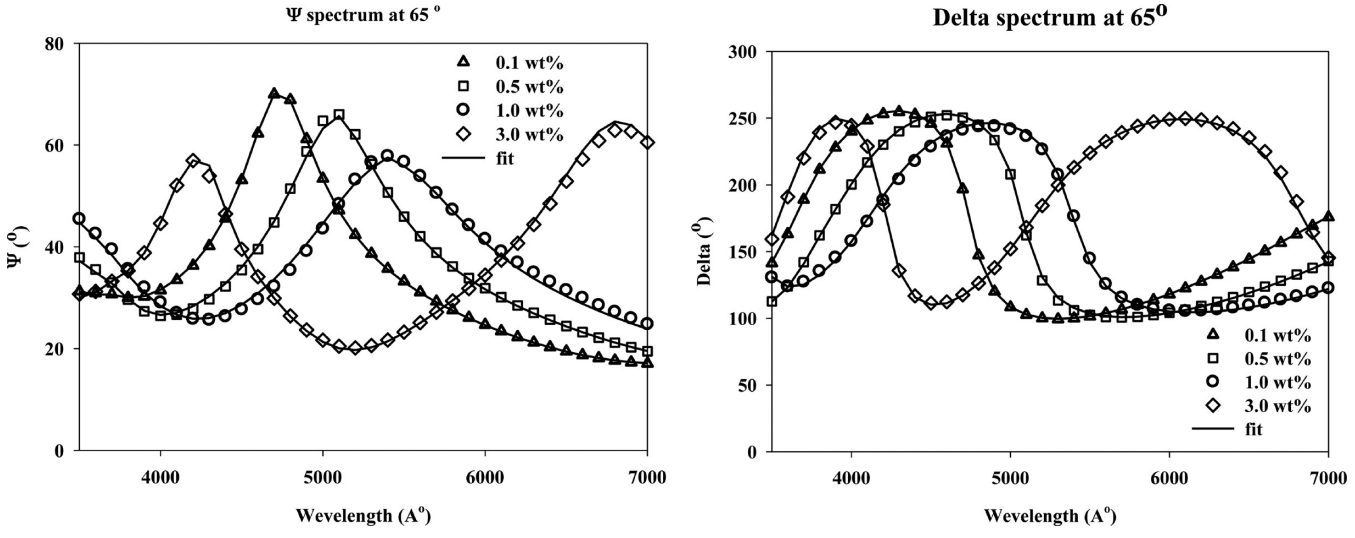

Figure 5. ψ and Δ spectra obtained from variable angle spectroscopic ellipsometry of 4 different films at 65° incident angle and corresponding fits with a Cauchy model.

dx.doi.org/10.1021/ma4002319 | Macromolecules 2013, 46, 3461−3475

inhomogeneities in the film. Starting from the general expression that describes the intensity of photoelectron lines (eq 2) as a function of position of the atom and the electron take off angle, one can consider the relationship between different species in the Nafion film and the underlying silica substrate.

$$I_i = \int_{z=0}^{z} G_i^0 \exp\left(-\frac{z}{\lambda \sin(\alpha)}\right) dz \quad (2)$$

In the above expression, I_i is the integrated area of a peak of interest normalized by its sensitivity factor and the instrument's transmission function, G_i^0 contains the photoemission cross section and atomic density for the element, λ is the electron inelastic mean free path, α is the takeoff angle, and z is the position of the emitting electron within the sample (where z = 0 corresponds to the film−air or film−vacuum interface). The simplest approach to calculate the film thickness is to consider the attenuation of a substrate peak (here Si from the underlying silica) due to the presence of the Nafion film. Integration of eq 1 between d (the film thickness) and infinity yields eq 3.

$$\frac{I_{Si}}{I_{Si,bulk}} = \sin(\alpha) \exp\left(-\frac{d}{\lambda \sin(\alpha)}\right) \quad (3)$$

where, $I_{Si,bulk}$ is the photoelectron intensity produced by a clean silica substrate. At normal takeoff angle (α = 90°), this expression is similar to a Beer−Lambert absorption equation, where the electrons produced by the silica substrate are attenuated by the Nafion film. Using this expression for the Si_{2p} intensities, the value of d/λ can be obtained (1.1758 and 2.8432 for the 0.1 and 0.25 wt % films, respectively). The film thickness can then be calculated directly by using λ = 3.7 nm. The value of the electron mean free path varies with electron kinetic energy and the composition and density of the medium though which it is traveling. The values chosen here were estimated by comparison with electrons of the same kinetic energy traveling though silica and several polymer films as quoted in the NIST database and calculated using the NIST standard reference database 71 software[50,51] for possible densities for the film. The calculations result in film thicknesses of 4.3 and 10.5 nm for the 0.1 and 0.25 wt % films, respectively, in excellent agreement with ellipsometry and AFM measurements (Table 2).

A second method was used to crosscheck the film thickness. Again, starting from eq 2, one can consider the intensities of Si_{2p} as the underlying substrate and S_{2p} as originating solely from the film. After integration, one can then consider the ratio of these intensities to calculate the film thickness. This methodology works well when the kinetic energies of the electrons considered is similar, and therefore the value of λ can be considered the same for both peaks (eq 4).

$$\frac{I_S}{I_{Si}} = \frac{I_{S,thick}}{I_{Si,bulk}} \left(e^{(d/[\lambda \sin \alpha])^{-1}}\right) \quad (4)$$

In this case, $I_{S,thick}$ is the intensity of sulfur in bulk Nafion, which was measured in the thick nafion films (3.0 wt %). The net result of this approach yields thicknesses of 4.1 and 9.6 nm for the 0.1 and 0.25 wt % films, respectively, within 10% of the simplest methodology. Some variation was indeed expected as the model assumes a film of homogeneous thickness and homogeneous distribution of the monitored species. Indeed, only a 10% discrepancy indicates these assumptions are reasonable. When the normalized XPS intensities obtained at 90° take off angle are plotted versus film thickness (inset of Figure 8), the profile is consistent with the expected exponential dependence. The profile is also consistent with the limit in probing depth of ∼15 nm, equivalent to 4 times λ, for these films.

Comparison of Thickness Determination by AFM, XPS, and Ellipsometry. The thickness of self-assembled Nafion films estimated using three different techniques is presented in Table 2. It is remarkable that three different techniques employing three different measurement principles yield similar results. The XPS technique is limited to estimating film thicknesses less than 3−4 times the attenuation length of electrons from the substrate. The attenuation lengths typically range 2−4 nm (λ = 3.7 nm for Si_{2p} electrons in this case), so films of thickness less than 16 nm only can be determined from XPS analysis. The surface roughness (discussed later) measurements from AFM indicate that the roughness is significantly lower than the lowest film thickness. This implies that no substrate area of any significant size remained uncovered and that the film completely covers the substrate. The roughness and surface feature size of Nafion films also confirm that the nonuniformity of films at relevant length scales is small.

Influence of the Solvent/Dispersion Media on Self-Assembled Films. The films characterized in the previous section were prepared by self-assembly from IPA-diluted Nafion dispersions of varying concentration. Upon dilution of stock solution by IPA, in addition to the change in Nafion concentration, the dispersion composition also changed. The nature of dispersion media is known to have significant and nonsignificant effect on the nanostructure including the aggregation state of Nafion in the dispersion. To delineate the concentration and dispersion media effects, a set of films was prepared from Nafion in water dispersions at same concentrations as that used for films from IPA-diluted dispersions. The thickness of films self-assembled from Nafion dispersion in water was determined by ellipsometry measurements. The results are presented in Table 2. It can be noted that all films generated from Nafion dispersion in water with concentrations ranging 0.25−5.0 wt % yield comparable thickness to those generated from IPA-diluted dispersions. One exception was the film self-assembled from the very dilute dispersion of 0.1 wt %. Further discussion on this film (0.1 wt % dispersion) is presented later in this section. The refractive index (RI) was obtained from the fit to ellipsometry data was similar with respect to thickness for the films prepared from the two different types of Nafion dispersions (figure RI vs thickness; see Supporting Information) . The similarity in refractive indices would indicate similarity of film structure. It can be inferred that the dispersion media (IPA vs water) has no significant impact on the self-assembly of the films for dispersions containing greater than 0.25 wt % Nafion.[52] The effect of dispersion media on self-assembly of Nafion films is apparent in the films prepared from highly diluted 0.1 wt % dispersions. We found scattered deposition of Nafion bundles or globules on the substrate from 0.1 wt % Nafion in water (assessed by AFM imaging; see Supporting Information) whereas the IPA-diluted 0.1 wt % dispersion yields a continuous film.

The similarity of thicknesses of the films prepared from similar concentrations (0.25−5.0 wt %) is very interesting to note. If the assembled Nafion maintains its agglomeration state in dispersion, then the similarity in thickness would indicate

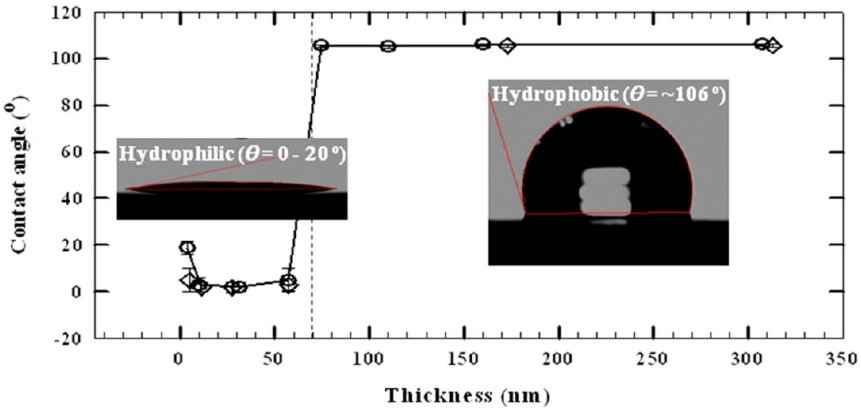

Figure 7. Water contact angle of ultrathin and thin Nafion films varying film thickness [open circles, films from IPA-diluted dispersions; open diamond, films from Nafion in water dispersions].

that the shape/size of Nafion in dispersion does not vary significantly between IPA-diluted and water-based dispersion. This would be supported by the studies of Nafion dispersion in alcohol and water where rod-like[33−36] or fringed rod like[37−39] Nafion exists and further agglomeration proceeds through the side chain interaction. Characterization of the dispersion is needed to answer whether aggregation of Nafion in IPA and water results in similar dimensions at a given concentration and whether it is the size of this aggregated state that is a controlling factor in the film thickness observed but that is beyond the scope of this study.

Surface Wettability by Water Contact Angle. To characterize the surface wettability, contact angle measurements with water were performed. The water contact angle of the blank substrate was determined to be 45°. The water contact angles for the films prepared from both IPA-diluted Nafion and Nafion-in-water dispersions and are presented in Figure 7. The images of sessile drops of water for 4 to 300 nm films prepared from IPA-diluted Nafion disperion are also shown in Figure 7.

Two important observations can be made from the data in Figure 7. First, all films except the thinnest (4 nm) exhibit either a very hydrophilic surface or a hydrophobic surface. Second, the films prepared from two different dispersions (in water and IPA-diluted) have nearly identical contact angles. Again, the latter observation supports the idea that Nafion concentration in the dispersion rather than the nature of the dispersion media affects the film properties. For the thinnest film (4 nm), a very low contact angle of 22° can be noted. The 10, 30, and 55 nm films exhibited highly hydrophilic behavior wherein the water droplet immediately spread upon placement as resulting almost zero contact angle. Remarkably, for the films thicker than 55 nm, a sudden jump in contact angle to around 106°, exhibiting hydrophobic behavior of the film surface, was observed. The high contact angle of around 106° is comparable to the values reported for Nafion membrane surfaces.[53,54] Furthermore, for the thicker films (>55 nm) the water droplet was stable as high contact angle did not break down small angle rather evaporates gradually by several hours. The contact angle for 4 nm film requires some comments. The measured contact angle of 22° is between that of the clean substrate (45°) and spreading behavior of the thicker films. A simplistic possibility is to think of the 4 nm film as partially covering the SiO_2 substrate resulting in a value that is intermediate of the contact angles of the two surfaces. On the other hand, AFM imaging of the substrate show complete coverage of the substrate. It is not possible to ascertain the contribution of the substrate to the measured contact angle for the 4 nm film. However, for the thicker films (10, 30, and 55 nm) the contact angle is spreading and not a nonzero value, which is a strong evidence that the substrate does not contribute to the measurements.

The hydrophilic free surface of sub-55 nm films and hydrophobic free surface of thicker samples (>55 nm films) is an indicator of changes in microdomain structure. It is interesting to note that in a recent study, Eastman et al.[30] have also observed that the properties of Nafion films of thickness less than 60 nm differ from those thicker than 60 nm. It would appear that 50−60 nm is an interesting length scale wherein perhaps the influence of substrate is still dominant resulting in a film with different free surface than the thicker films. The latter films have a free surface that is similar to those of bulk membranes.

Given that Nafion is made of hydrophobic Teflon-like backbone and a hydrophilic sulfonic acid terminated side chain, it is natural to assign the hydrophilic behavior to the orientation of the hydrophilic sulfonic groups toward the air−film interface arising from an ordered structure in the thin films. In contrast, the Nafion membrane surface is known to exhibit hydrophobic behavior[24] attributable to the random structure of the membrane such that largely hydrophobic fluorocarbon backbones present itself to the air−film or air−membrane surface.

Surface Morphology of Films Varying in Thickness. The surface morphology of these films was examined by AFM to investigate whether the surface of the sub-55 nm and thicker (>55 nm) films showed any differences. Here, the results for films generated from IPA-diluted dispersions only are presented. The AFM images of films generated from from Nafion dispersion in water are available as Supporting Information. The height and corresponding phase contrast images obtained from AFM measurements are presented in Figure 8. Each of the phase and topographical image is accompanied by a line analysis to provide an insight into the distribution of the pertinent feature—phase shift angle or height. The root-mean-square (RMS) deviation of the pertinent feature is also indicated on the images. For the height/topography images, the RMS value represents the mean roughness as per the definition in eq 1. For the phase contrast, an equivalent expression applies where the height is replaced with phase shift angle.

The topography images do not reveal any periodic or clear features. The root-mean-square surface roughness (R_{rms}) was

dx.doi.org/10.1021/ma4002319 | Macromolecules 2013, 46, 3461−3475

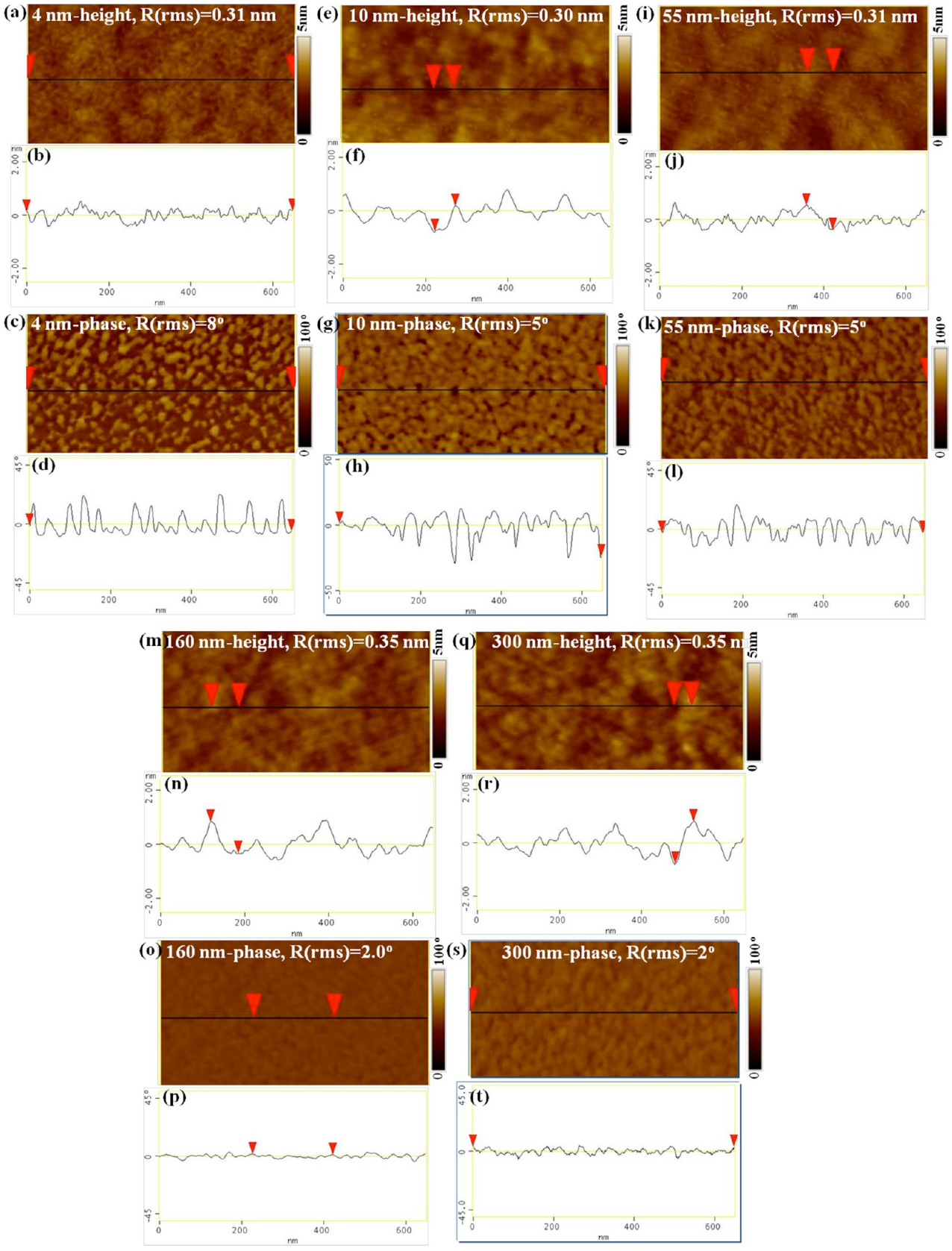

Figure 8. Height and corresponding phase images with section analysis of 4 nm film (a, b, c, d), 10 nm film (e, f, g, h), 55 nm film (i, j, k, l), 160 nm film (m, n, o, p), and 300 nm film (q, r, s, t). [Films prepared from IPA-diluted Nafion dispersions].

found to increase only slightly from 0.31 nm for 4 nm film to 0.35 nm for 300 nm film. No significant differences in the surface roughness of thinner hydrophilic and thicker hydrophobic films exist. The examination of the phase images

dx.doi.org/10.1021/ma4002319 | *Macromolecules* 2013, 46, 3461−3475

indicate connected fiber-like features for the ultrathin films (<55 nm). The features in the phase images of thicker (160 and 300 nm) films are less clear, perhaps indicative of a more random orientation. Phase contrast can arise from inhomogeneity in physical (height), chemical (hydrophilicity/hydrophobicity), or mechanical (film modulus or hardness) properties of the film. The latter two arise from interaction between the tip and the film. Comparing the phase image and topographical images, it is evident that there is no obvious correlation between the two. As such, we attribute the features in the phase contrast images to arise from differences in the interaction (film modulus or hydrophilic/hydrophobic) of the AFM tip with different local chemical nature of the film.

To investigate whether some statistical parameters such as surface roughness could be correlated to the observed differences in the wettability, we analyzed the root-mean-square deviation of phase shift angle. The use of phase contrast of Nafion membrane as a metric of surface wettability has been reported by James et al.[55]

The trend we note is that the RMS deviation of phase angle for hydrophilic films are greater than 5° whereas that for the hydrophobic films (160 and 300 nm) are only 2°. Incidentally the *mean* phase shift angle of all the films are all within 0.5 degrees of each other. However, the RMS deviations differ for the films indicating that the distribution of the phase shift angles differ. It appears that RMS deviation of phase shift angles may be an interesting measure for characterizing the differences in wettability of Nafion films. However, further investigation is required to establish a clear correlation and is beyond the scope of the present study.

Compositional Homogeneity of Films by Angle-Resolved XPS. To explore whether the surface of thinner films were enriched with sulfonic groups and that of thicker films enriched with fluorocarbon backbones, we carried out angle-resolved XPS. For this purpose, representative peaks can be taken from the side chain and backbone, such that if layering is present in the films, these elements will show different angular distributions. We used the S_{2p} peak that originates from the nafion side chains and the F_{1s} peak, which originates predominantly from the backbone. Table 3 shows the integrated areas for these elements (corrected for transmission function and sensitivity factors). The C_{1s} peak is also shown as reference.

The ratio of S to F concentrations appears to be constant for the thicker films, but an apparent increase in this ratio is observed for the ultrathin film as the takeoff angle decreases.

Table 3. Angle-Resolved XPS Data for Three Different Films

nominal film thickness (nm)	angle (deg)	absolute intensities S	F	C	I_S/I_F	G_S/G_F
4	90	433.2	19429.7	11166.1	0.0230	0.0192
	45	250.0	9221.9	5875.0	0.0271	0.0225
	10	94.4	3345.4	2591.6	0.0282	0.0214
10	90	490.4	15646.3	9624.6	0.0313	0.0246
	40	299.8	9479.1	6280.6	0.0316	0.0235
	10	179.8	6370.4	4251.4	0.0282	0.0201
160	90	680.4	20868.6	14338.9	0.0326	0.0247
	45	337.0	10332.4	7894.6	0.0326	0.0247
	10	101.6	3227.2	2649.7	0.0315	0.0238

Such change could be associated with a structure in which there is an ordering of the nafion side chains in the top layer of the film (S rich). This interpretation is very tempting as it may account for the slightly more hydrophilic nature of the ultrathin film. However, a complete analysis of the ARXPS should consider the difference in the electron mean free path between the F_{1s} and S_{2p} electrons (λ = 2.8 and λ = 3.7 nm, respectively). The relationship is shown in eq 5, where the stoichiometric ratio is represented by G_S/G_F.

$$\frac{I_S}{I_F} = \frac{G_S\lambda_S}{G_F\lambda_F}\left(\frac{1 - e^{-(d/[\lambda_S \sin \alpha])}}{1 - e^{-(d/[\lambda_F \sin \alpha])}}\right) \quad (5)$$

Upon correcting the data for the mean free path length of F_{1s} and S_{2p} electrons, according to eq 5, we find that the actual stoichiometric ratio between the side chains and the backbone is constant for all the films. That is, within the error of the measurements, the heterogeneity within the films cannot be ascertained. On the basis of these results, we did not pursue AR-XPS investigation of films generated from water-based dispersions.

XDLVO Surface Energy Calculations. Surface energy of the films can be a useful data for understanding and modeling of interaction between the Nafion film surface and other fluids and solids. Such information may also be useful to characterizing the interaction between Nafion in dispersion and a substrate. In this work, we use the extended DLVO theory (or XDLVO for brevity) for the determination of surface energy. In the XDLVO or the Lewis acid–base model, introduced by Good,van Oss, and Chaudhury,[56] the surface energy components of a solid surface can be obtained from measuring the contact angles made by liquid triplets on that surface. Usually two polar liquids (e.g., water, ethylene glycol) and one apolar liquid (e.g., diiodomethane, α-bromonaphthalene) are used. Conceptually,[57,58] the total surface energy (γ_S^{Tot}) is the sum of a Lifshitz-van der Waals (γ_S^{LW}) component and an acid–base component (γ_S^{AB}). The acid–base component can be further defined by an electron-donating (γ_S^-) and an electron accepting parameter (γ_S^+), expressed as follows:

$$\gamma_S^{Tot} = \gamma_S^{LW} + \gamma_S^{AB} \quad (6)$$

where,

$$\gamma_S^{AB} = 2\sqrt{\gamma_S^+\gamma_S^-} \quad (7)$$

It is useful to point out that the both the Lewis acid–base (electron donating/accepting) and Bronsted acid–base (proton donating/accepting) interactions are lumped in the acid–base (AB) component of the surface energy parameters. For Nafion, these parameters may be better understood in terms of proton donating/accepting properties. Using liquids of known surface energy parameters (here, water, ethylene glycol and diiodomethane) and measuring the contact angles they make on the Nafion film surface, the surface energy parameters of the latter can be calculated through regression of the measured contact angle data according to the following model equation.[59]

$$(1 + \cos\theta)\gamma_L^{Tot} = 2\left(\sqrt{\gamma_L^{LW}\gamma_S^{LW}} + \sqrt{\gamma_L^+\gamma_S^-} + \sqrt{\gamma_L^-\gamma_S^+}\right) \quad (8)$$

In addition to the 4 and 160 nm Nafion films, measurements were carried out on Teflon as an internal reference. Contact angles measured using three different liquids of varying polarity are reported in Table 4. The surface energy components were

dx.doi.org/10.1021/ma4002319 | Macromolecules 2013, 46, 3461–3475

Table 4. Calculated Surface Energy of the Adsorbed Thin Nafion Films According to the XDLVO Theory[a]

material	θ_w (deg)	θ_d (deg)	θ_e (deg)	θ_f (deg)	γ^{LW} (mJ/m^2)	$\gamma^{\oplus}$ (mJ/m^2)	$\gamma^{\ominus}$ (mJ/m^2)	γ^{Tot} (mJ/m^2)
4 nm film	21.6 ± 3.8	85.3 ± 1.2	15.9 ± 2.3	–	14.0	5.2	66.6	51.2
160 nm film	106.1 ± 0.6	86.3 ± 0.6	97.8 ± 0.7	–	14.1	0.5	5.8	17.5
Teflon (in house)	115.3	85.6	–	107.0	14.6	0.8	2.2	17.2
Teflon (literature)[64]					14.7–25.8	0.0–0.3	0.0–3.0	14.7–26.0
Nafion membrane[60]					12.7	0.1	6.0	14.2

[a] θ_w, θ_d, θ_e and θ_f represent contact angle measurement using water, diiodomethane, ethylene glycol and formaldehyde, respectively.

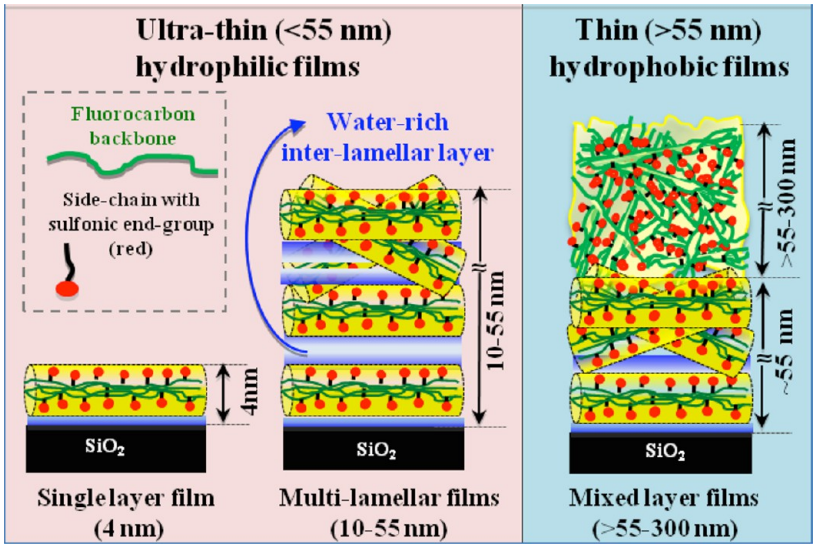

Figure 9. Thickness –dependent proposed nanostructure of ultrathin and thin Nafion films.

calculated by matrix solution using Matlab for the 4 and 160 nm Nafion films and the Teflon are also presented in Table 4. Repeat measurements on multiple samples (3 or more) of 4 and 160 nm films were made and exhibited the noted hydrophilic and hydrophobic behavior, respectively. Measurements made on 3–4 different locations on each of the 4 repeat samples yielded the average value reported in Table 4.

The intermediate thickness films were not assessed since, in the hydrophilic limit, the spreading water makes the small contact angle measurement inaccurate. The surface energy parameters for the liquids were obtained from literature.[61] Surface energies of Teflon or poly(tetrafluoroethylene) determined from measurements in our laboratory yield values within the range reported in literature. The surface energy components of the 160 nm film are comparable to that of the Teflon but slightly higher than those of Nafion membrane surface energies reported by Kim et al.[60] On the other hand, the total surface energy of the 4 nm film is more than three time higher than that of the 160 nm film as well as the Nafion membrane. Interestingly, a high value of the electron accepting parameter (66.0 mJ/m^2) for the 4 nm film indicates that the surface is highly polar. This high polarity might be attributed due to presence of higher number of hydrophilic sulfonate groups at the surface. Furthermore, the van der Waal components of all films have a value comparable to the 14.6 mJ/m^2 value for Teflon. The total surface energy of 160 nm film is close to that of the Teflon surface (17.2 mJ/m^2) measured by the same method. This is expected since the Teflon-like backbone of Nafion should dominate the van der Waal's interaction with the test liquid. The exact reason for the Teflon and 160 nm film possessing higher surface energy than literature reported Nafion membrane is not clear. One possibility is the difference arising from the variability in the measurement conditions and the experimental setup. Further differences may arise because for Nafion membrane the surface energy could possibly be a function of membrane thickness. Nonetheless, the results support that the XDLVO type analyses offer useful insight into nature of interaction of Nafion with other liquids and even other surfaces.

Proposed Nanostructure of Self-Assembled Nafion Films. We propose a thickness-dependent structure of the self-assembled films as depicted in Figure 9.

Our thinnest film (4 nm) is the most interesting one not only because of the relevance of the length scale to the ionomer thickness observed in PEFC catalyst layer but because the thickness is remarkably close to the diameter of rod-like Nafion aggregate observed in hydro-alcoholic solution by small angle scattering experiments.[33–35,62,63] The hydrophilic character of the free surface of these films, demonstrated by spreading of water droplet, is also consistent with the proposed structure of the Nafion bundles/rods in hydro-alcoholic solutions with sulfonic side chains protruding outward. For the side of the film interfacing with the substrate, Nafion likely interacts via hydrogen bonding with the thin hydration layer formed on the SiO_2 surface. We do not have a direct proof of whether the bundle-like structure remains intact or it opens up upon adsorption on SiO_2. However, given the coincidental thickness of the 4 nm film with the reported diameter of Nafion bundles in hydro-alcoholic solutions/dispersions as well as the hydrophilic nature of the free surface, it is plausible that the 4 nm film is made of largely of rods or bundles lying flat on the substrate. However, we have not been able to confirm this. Characterization of our films by GISAXS has not revealed any discernible features or the presence of ionomer domains.[52] In Figure 9, a

dx.doi.org/10.1021/ma4002319 | Macromolecules 2013, 46, 3461–3475

water-rich interfacial structure (between Nafion and SiO_2) is depicted. This idea is derived from and consistent with the neutron reflectometry work by the NIST group[18,19] and that proposition by Hickner group.[28]

For 10−55 nm films, a lamellar structure similar to that proposed by Dura et al.[19] seems to be plausible. The polymer-rich lamellas can either be made of rods or bundles have the sulfonic-group containing side-chains extending outward or of less ordered structure. It can be argued that the free interface has significant sulfonic group density resulting in a hydrophilic film surface. The water in the interlamellar layers would have to come from tightly bound hydration shell that forms around the sulfonic group. The water would also be responsible for shielding the repulsive forces arising from the interaction of the sulfonic groups in the two lamellas. It is likely that the 30 and 55 nm have some bundles oriented at an intermediate angle between zero and 90 degrees.

For the 160 and 300 nm, the hydrophobic free surface suggests that the surface structure of the films is similar to those of the membrane. Bass et al.[24] have proposed from their GISAXS study of 100 nm films formed on OTS-modified SiO_2 surface that a majority of the Nafion bundles near the free interface would have to orient vertically to the substrate consistent with a hydrophobic surface. The nature or structure of the film near the SiO_2−Nafion interface may be multi-lamellar as has been noted by Dura et al.[19] from Neutron Reflectometry measurements, albeit on a spin-coated film.

CONCLUSIONS

In this study, we examined the surface characteristics of self-assembled films of Nafion, on thermally grown on SiO_2 substrate, generated by immersion in Nafion solution of different concentrations. The thickness of the resulting films were found to increase with increasing Nafion solution concentrations, ranging from 4 nm for films generated from a 0.1 wt % solution to 300 nm for films generated from 5 wt % solutions. Consistent film thicknesses were obtained by three different techniques − XPS, AFM and Ellipsometry. The 4 nm film is one of *thinnest, continuous films* of Nafion ever reported. The film thickness is of the same length scale as that reported for diameter of rod-like or fibrillar structure of Nafion in polar solvent. One of the interesting findings of the study was thickness-dependent wettability of the films. The ultrathin films (<55 nm) showed hydrophilic surface characteristics whereas the thicker films (>55 nm) showed hydrophobic surface characteristics. The hypothesized sulfur-rich surface of thinner films was investigated with angle-resolved XPS and apparent enrichment in S/F ratio was noted. However, upon accounting for the angle effects and mean free path lengths of pertinent S and F electrons, the S/F ratio of all films was found to fall within the variance of the experimental measurements. Nonetheless, differences in surface features as noted in AFM-phase image and surface wettability between the ultrathin (<55 nm) and thin (>55 nm) films indicate that ultrathin films have structure and properties are distinct from the thicker films, which exhibit characteristics similar to that of free-standing membrane form of Nafion.

Many factors are expected to influence the structure and properties of the films including the preparation methods (self-assembly, spin-coating, drop casting) and the surface chemistry of the substrate. It is expected that the substrate surface chemistry will play an important role in the organization of polymer molecules on the surface, as such the conclusions drawn here must be restricted to Nafion films on SiO_2 substrate. Extrapolation of the findings to platinum or carbon substrates, pertinent to fuel cells, would be purely hypothetical at this stage given the differences in structure reported by Dura et al.[19] and Wood et al.[20]

Nonetheless, new findings on Nafion thin films including the results from this study offer the cautionary note that the assumption of these films possessing similar properties as well-studied and characterized Nafion membrane could result in serious errors. As with Nafion membrane, a thorough understanding of all the influencing factors and a generalized law describing the interactions of Nafion with substrates in different dispersion media will require extensive and multi-technique characterization of thin films of this interesting material.

ASSOCIATED CONTENT

Supporting Information

Nafion−water dispersion preparation procedure, the ellipsometry fitting results, comparative ellipsometry raw data, refractive index data of both type of films obtained from IPA diluted dispersion and water dispersion of Nafion, and AFM images of the film prepared from Nafion−water dispersion. This material is available free of charge via the Internet at http://pubs.acs.org/.

AUTHOR INFORMATION

Corresponding Author

*(K.K.) E-mail: kkaran@ucalgary.ca. Telephone: 1-403-220-5754. Fax: 1-403-284-4852.

Present Addresses

‡(K.K.) Department of Chemical and Petroleum Engineering, The University of Calgary, Calgary, Canada

∥(J.P.) Department of Materials Science & Engineering and Department of Electrical & Computer Engineering, Michigan Technological University, Houghton, MI 49931

Notes

The authors declare no competing financial interest.

ACKNOWLEDGMENTS

The financial assistance for this work was provided by the Natural Sciences and Engineering Research Council of Canada (NSERC) and the Early Researcher Award (for K.K.), Ontario Ministry of Research.

REFERENCES

(1) Heitner-Wirguin, C. Recent advances in perfluorinated ionomer membranes: structure, properties and applications. *J. Membr. Sci.* **1996**, *120*, 1−33.

(2) Choi, P.; Jalani, H. N.; Datta, R. Thermodynamics and Proton Transport in Nafion II. Proton Diffusion Mechanisms and Conductivity. *J. Electrochem. Soc.* **2005**, *152*, E123−E130.

(3) Yeo, S. R.; McBreen, J.; Kissel, G.; Kulesa, F.; Srinivasan, S. Perfluorosulphonic acid (Nafion) membrane as a separator for an advanced alkaline water electrolyser. *J. Appl. Electrochem.* **1980**, *10*, 741−747.

(4) Grot, W. *Chem. Ing. Tech.* **1978**, *50*, 299−301.

(5) Tailoka, F.; Fray, D. J.; Kumar, R. V. Application of Nafion electrolytes for the detection of humidity in a corrosive atmosphere. *Solid State Ionics* **2003**, *161*, 267−277.

(6) More, K.; Borup, R.; Reeves, K. Identifying Contributing Degradation Phenomena in PEM Fuel Cell Membrane Electride Assemblies Via Electron Microscopy. *ECS Trans.* **2006**, *3*, 717−733.

(7) Mauritz, K. A.; Moore, R. B. State of Understanding of Nafion. *Chem. Rev.* **2004**, *104*, 4535−4586.
(8) Schmidt-Roh, K.; Chen, Q. Parallel cylindrical water nanochannels in Nafion fuel-cell membranes. *Nat. Mater.* **2008**, *7*, 75−83.
(9) Gebel, G.; Diat, O. Neutron and X-ray Scattering: Suitable Tools for Studying Ionomer Membranes. *Fuel Cells* **2005**, *5*, 261−276.
(10) Blanchard, R. M.; Nuaao, G. R. An Infrared Study of the Effects of Hydration on Cation-Loaded Nafion Thin Films. *J. Polym. Sci. Part B: Polym. Phys.* **2000**, *38*, 1512−1520.
(11) Krtil, P.; Trojánek, A.; Samec, Z. Kinetics of Water Sorption in NafionThin Films - Quartz Crystal Microbalance Study. *J. Phys. Chem. B* **2001**, *105*, 7979−7983.
(12) Hill, A. T.; Carroll, L. D.; Czerw, R.; Martin, W. C.; Perahia, D. Atomic Force Microscopy Studies on the Dewetting of Perfluorinated Ionomer Thin Films. *J. Polym. Sci., Part B: Polym. Phys.* **2003**, *41*, 149−158.
(13) Siroma, Z.; Ioroi, T.; Fujiwara, N.; Yasuda, K. Proton conductivity along interface in thin cast film of Nafion. *Electrochem. Commun.* **2002**, *4*, 143−145.
(14) Bertoncello, P.; Ugo, P. Preparation and Voltammetric Characterization of Electrodes Coated with Langmuir-Schaefer Ultrathin Films of Nafion. *J. Braz. Chem. Soc.* **2003**, *14*, 517−522.
(15) Ugo, P.; Bertoncello, P.; Vezzà, F. Langmuir−Blodgett films of different ionomeric polymers deposited on electrode surfaces. *Electrochim. Acta* **2004**, *49*, 3785−3793.
(16) Bertoncello, P.; Ciani, I.; Li, F.; Unwin, R. P. Measurement of Apparent Diffusion Coefficients within Ultrathin Nafion Langmuir-Schaefer Films: Comparison of a Novel Scanning Electrochemical Microscopy Approach with Cyclic Voltammetry. *Langmuir* **2006**, *22*, 10380−10388.
(17) Umemura, K.; Wang, T.; Hara, M.; Kuroda, R.; Uchida, O.; Nagai, M. Nanocharacterization and Nanofabrication of a Nafion Thin Film in Liquids by Atomic Force Microscopy. *Langmuir* **2006**, *22*, 3306−3312.
(18) Murthi, V. S.; Dura, J. A.; Satija, S.; Majkrzak, C. F. Water Uptake and Interfacial Structural Changes of Thin Film Nafion® Membranes Measured by Neutron Reflectivity for PEM Fuel Cells. *ECS Trans.* **2008**, *16*, 1471−1485.
(19) Dura, A. J.; Murthi, S. V.; Hartman, M.; Satija, K. S.; Majkrzak, F. C. Multilamellar Interface Structures in Nafion. *Macromolecules* **2009**, *42*, 4769−4774.
(20) Wood, L. D.; Chlistunoff, J.; Majewski, J.; Borup, L. R. Nafion Structural Phenomena at Platinum and Carbon Interfaces. *J. Am. Chem. Soc.* **2009**, *131*, 18096−18104.
(21) Noguchi, H.; Taneda, K.; Minowa, H.; Naohara, H.; Uosaki, K. Humidity-Dependent Structure of Surface Water on Perfluorosulfonated Ionomer Thin Film Studied by Sum Frequency Generation Spectroscopy. *J. Phys. Chem. C* **2010**, *114*, 3958−3961.
(22) Siroma, Z.; Kakitsubo, R.; Fujiwara, N.; Ioroi, T.; Yamazaki, S.-I.; Yasuda, K. Depression of proton conductivity in recast Nafion film measured on flat substrate. *J. Power Sources* **2009**, *189*, 994−998.
(23) Bass, M.; Berman, A.; Singh, A.; Konovalov, O.; Freger, V. Surface Structure of Nafion in Vapor and Liquid. *J. Phys. Chem. B* **2010**, *114*, 3784−3790.
(24) Bass, M.; Berman, A.; Singh, A.; Konovalov, O.; Freger, V. Surface-Induced Micelle Orientation in Nafion Films. *Macromolecules* **2011**, *44*, 2893−2899.
(25) Paul, D. K.; Fraser, A.; Karan, K. Towards the understanding of proton conduction mechanism in PEMFC catalyst layer: Conductivity of adsorbed Nafion films. *Electrochem. Commun.* **2011**, *13*, 774−777.
(26) Kongkanand, A. Interfacial Water Transport Measurements in Nafion Thin Films Using a Quartz-Crystal Microbalance. *J. Phys. Chem. C* **2011**, *115*, 11318−11325.
(27) Ahmed, M.; Morgan, D.; Attard, A. G.; Wright, E.; Thompsett, D. Sharman, Unprecedented Structural Sensitivity toward Average Terrace Width: Nafion Adsorption at Pt{*hkl*} Electrodes. *J. Phys. Chem. C* **2011**, *115*, 17020−17027.
(28) Dishari, K. S.; Hickner, M. A. Antiplasticization and Water Uptake of Nafion Thin Films. *ACS Macro Lett.* **2012**, *1*, 291−295.
(29) Modestino, M. A.; Kusoglu, A.; Hexemer, A.; Weber, A. Z.; Segalman, R. A. Controlling Nafion Structure and Properties via Wetting Interactions. *Macromolecules* **2012**, *45*, 4681−4688.
(30) Eastman, S. A.; Kim, S.; Page, K. A.; Rowe, B. W.; Kang, S.; Soles, C. L. Effect of Confinement on Structure, Water Solubility, and Water Transport in Nafion Thin Films. *Macromolecules* **2012**, *45*, 7920−7930.
(31) Stafford, C. M.; Vogt, B. D.; Harrison, C.; Julthongpiput, D.; Huang, R. Elastic Moduli of Ultrathin Amorphous Polymer Films. *Macromolecules* **2006**, *39*, 5095−5099.
(32) Iden, H.; Ohma, A.; Shinohara, K. Analysis of Proton Transport in Pseudo Catalyst Layers. *J. Electrochem. Soc.* **2009**, *156*, B1078−B1084.
(33) Aldebert, P. B. D. Rod like micellar structures in perfluorinated ionomer solutions. *J. Phys. (Paris)* **1988**, *49*, 2101−2109.
(34) Loppinet, B.; Gebel, G.; Williams, C. E. Small-Angle Scattering Study of Perfluorosulfonated Ionomer Solutions. *J. Phys. Chem. B* **1997**, *101*, 1884−1892.
(35) Gebel, G.; Loppinet, B. Colloidal structure of ionomer solutions in polar solvents. *J. Mol. Struct.* **1996**, *383*, 43−49.
(36) Aldebert, P.; Dreyfus, B.; Pineri, M. Small-Angle Neutron Scattering of Perfluorosulfonated Ionomers in Solution. *Macromolecules* **1986**, *19*, 2651−2653.
(37) Jiang, S.; Xia, K-Q.; Xu, G. Effect of Additives on Self-Assembling Behavior of Nafion in Aqueous Media. *Macromolecules* **2001**, *34*, 7783−7788.
(38) Lee, S.-J.; Yu, T. L.; Lin, H.-L.; Liu, W.-H.; Lai, C.-L. Solution properties of Nafion in methanol/water mixture solvent. *Polymer* **2004**, *45*, 2853−2862.
(39) Lin, H-L.; Yu, L. T.; Huang, C-H.; Lin, T.-L. Morphology study of Nafion membranes prepared by solutions casting. *J. Polym. Sci.: Part B: Polym. Phys.* **2005**, *43*, 3044−3057.
(40) Ma, C.-H.; Yu, T. L.; Lin, H.-L.; Huang, Y.-T.; Chen, Y.-L.; Jeng, U.-S. Morphology and properties of Nafion membranes prepared by solution casting. *Polymer* **2009**, *50*, 1764−1777.
(41) Ngo, T. T.; Yu, T. L.; Lin, H.-L. Influence of the composition of isopropyl alcohol/water mixture solvents in catalyst ink solutions on proton exchange membrane fuel cell performance. *J. Power Sources* **2013**, *225* (1), 293−303.
(42) Moore, R. B., 111; Martin, C. R. *Macromolecules* **1988**, *21*, 1334−1339.
(43) Chao, S. S.; Takagi, Y.; Lukovsky, G.; Pai, P.; Caster, R. C.; Tyler, J. T.; Keem, J. E. Chemical states study of Si in SiO_x films grown by PECVD. *Appl. Surf. Sci.* **1986**, *26*, 575−583.
(44) Reichl, R.; Gaukler, K. H. XPS Study of the Y/SiOx Interface at Room. Temperature. *Surf. Interface Anal.* **1990**, *15*, 211−214.
(45) NIST X-ray Photoelectron Spectroscopy Database, Version 3.5; National Institute of Standards and Technology: Gaithersburg, MD, 2003; http://srdata.nist.gov/xps/, (accessed January 2011).
(46) Fairley, N. CASA XPS version 2.3.13 Dev73, 2007.
(47) Hansma, H.; Motamedi, F.; Smith, P.; Hansma, P.; Wittman, J. C. Molecular resolution of thin, highly oriented poly (tetrafluoroethylene) films with the atomic force microscope. *Polymer* **1992**, *33*, 647−649.
(48) Lobo, R. F. M.; Pereira-da-Silva, M. A.; Raposo, M.; Faria, R. M.; Oliveira, O. N., Jr; Pereira-da-Silva, M. A.; Faria, R. M. In situ thickness measurements of ultra-thin multilayer polymer films by atomic force microscopy. *Nanotechnology* **1999**, *10*, 389.
(49) Paul, D. K.; Fraser, A.; Pearce, J.; Karan, K. Understanding the Ionomer Structure and the Proton Conduction Mechanism in PEFC Catalyst Layer: Adsorbed Nafion on Model Substrate. *ECS Trans.* **2011**, *41*, 1393−1406.
(50) Power, C. J.; Jablonski, A. Evaluation of Calculated and Measured Electron Inelastic Mean Free Paths Near Solid Surfaces. *J. Phys. Chem.* **1999**, *28*, 19−62.
(51) Jablonski, A. *NIST electron inelastic mean free path database v. 1.2*; NIST Standard Reference Database 71; U.S. Secretary of Commerce: Washington,. DC, 2010.

(52) Modestino, M. A.; Paul, D. K.; Dishari, S.; Petrina, S. A.; Allen, F. I.; Hickner, M. A.; Karan, K.; Segalman, R. A.; Weber, A. Z. Self-assembly and transport limitations in confined Nafion films. *Macromolecules* **2013**, *46* (3), 867−873.
(53) Zawodzinski, T. A.; Gottesfeld, S.; Shoichet, S.; McCarthy, T. J. The Contact-Angle between Water and the Surface of Perfluorosulfonic Acid Membranes. *J. Appl. Electrochem.* **1993**, *23*, 86−88.
(54) Goswami, S.; Klaus, S.; Benziger, J. Wetting and Absorption of Water Drops on Nafion Films. *Langmuir* **2008**, *24*, 8627−8633.
(55) James, P. J.; Antognozzi, M.; Tamayo, J.; McMaster, T. J.; Newton, J. M.; Miles, M. J. Interpretation of Contrast in Tapping Mode AFM and Shear Force Microscopy. A Study of Nafion. *Langmuir* **2001**, *17*, 349−360.
(56) Van Oss, C. J. *Interfacial Forces in Aqueous Media*: Marcel Dekker: New York, 1994.
(57) Bellon-Fontaine, M. N.; Mozes, N.; Van der, M. H. C.; Sjollema, J.; Cerf, O.; Rouxhet, P. G. *Cell Biophys* **1990**, *17*, 93−106.
(58) Sharma, P. K.; Rao, K. H. Analysis of different approaches for evaluation of surface energy of microbial cells by contact angle goniometry. *Adv. Colloids Interface Sci.* **2002**, *98*, 341−463.
(59) Van Oss, C. J. Development and applications of the interfacial tension between water and organic or biological surfaces. *Colloids Surf. B: Biointerfaces* **2007**, *54*, 2−9.
(60) Kim, Y.-H.; Oblas, D.; Angelopoulos, P. A.; Fossey, S. A.; Matienzo, J. L. *Macromolecules* **2001**, *34*, 7489.
(61) Good, R. J.; Van Oss, C. J. *Modern Approaches to Wettability Theory and Application*; Schader, M. E., Loeb, G. I., Eds.; Plenum Press: New York, 1992.
(62) Loppinet, B.; Gebel, G. Rod-like Colloidal Structure of Short Pendant Chain Perfluorinated Ionomer Solutions. *Langmuir* **1998**, *14*, 1977−1983.
(63) Rubatat, L.; Gebel, G.; Diat, O. Fibrillar Structure of Nafion: Matching Fourier and Real Space Studies of Corresponding Films and Solutions. *Macromolecules* **2004**, *37*, 7772−7783.
(64) Surface Energy Data for PTFE: Polytetrafluoroethylene, CAS # 9002-84-0, retrieved on 24th March, 2013 from the website. http://www.accudynetest.com/polymer_surface_data/ptfe.pdf